Supporting Information

Liquid crystalline phases from polymer functionalized ferri-magnetic Fe_3O_4 nanorods

B. Klöckner,[a] P. Daniel,[b] M. Brehmer,[a] W.Tremel[b] and R. Zentel*[a]

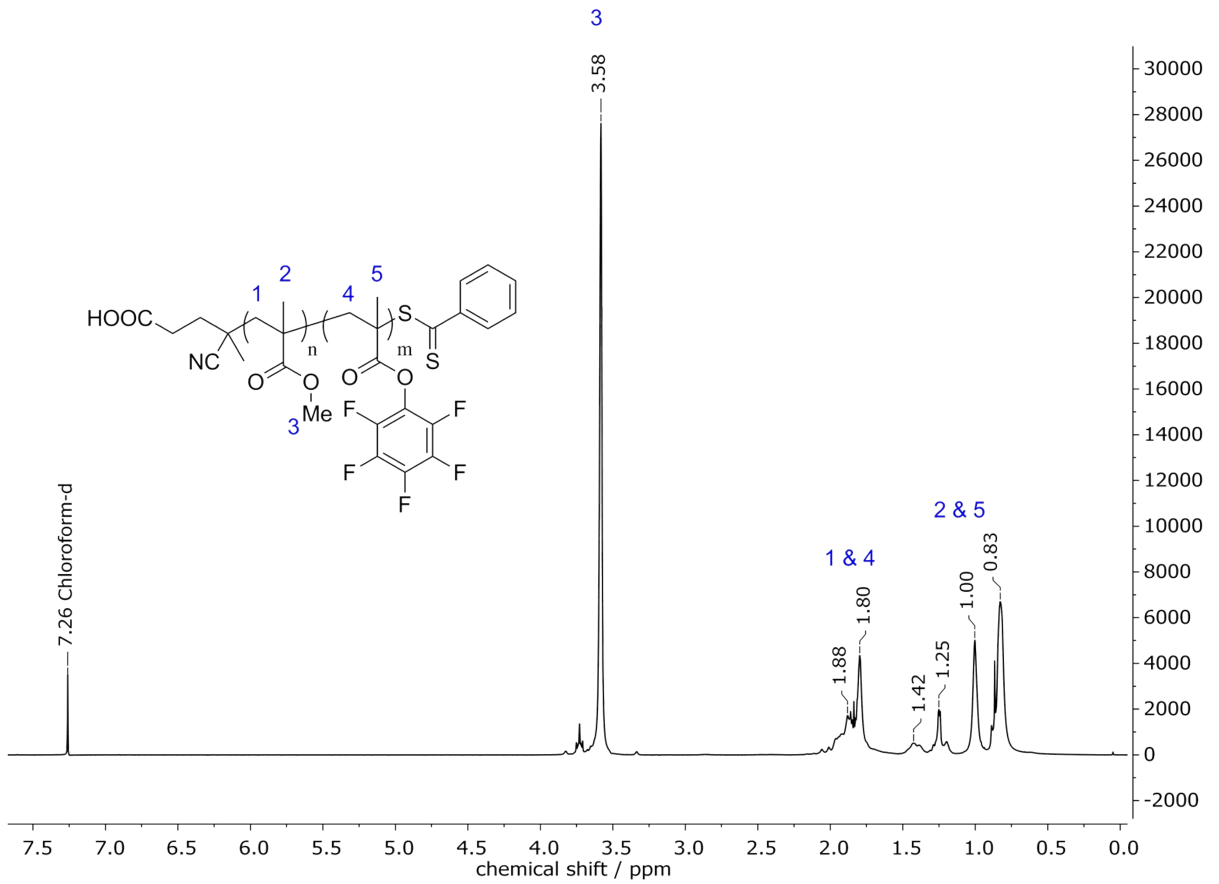

Figure S1: ^{1}H-NMR of reactive ester block copolymer P(MMA-*b*-PFPMA). The ratio between the PMMA block and the PFPMA-block was determined to be 9.1:1 by using ref. 1.

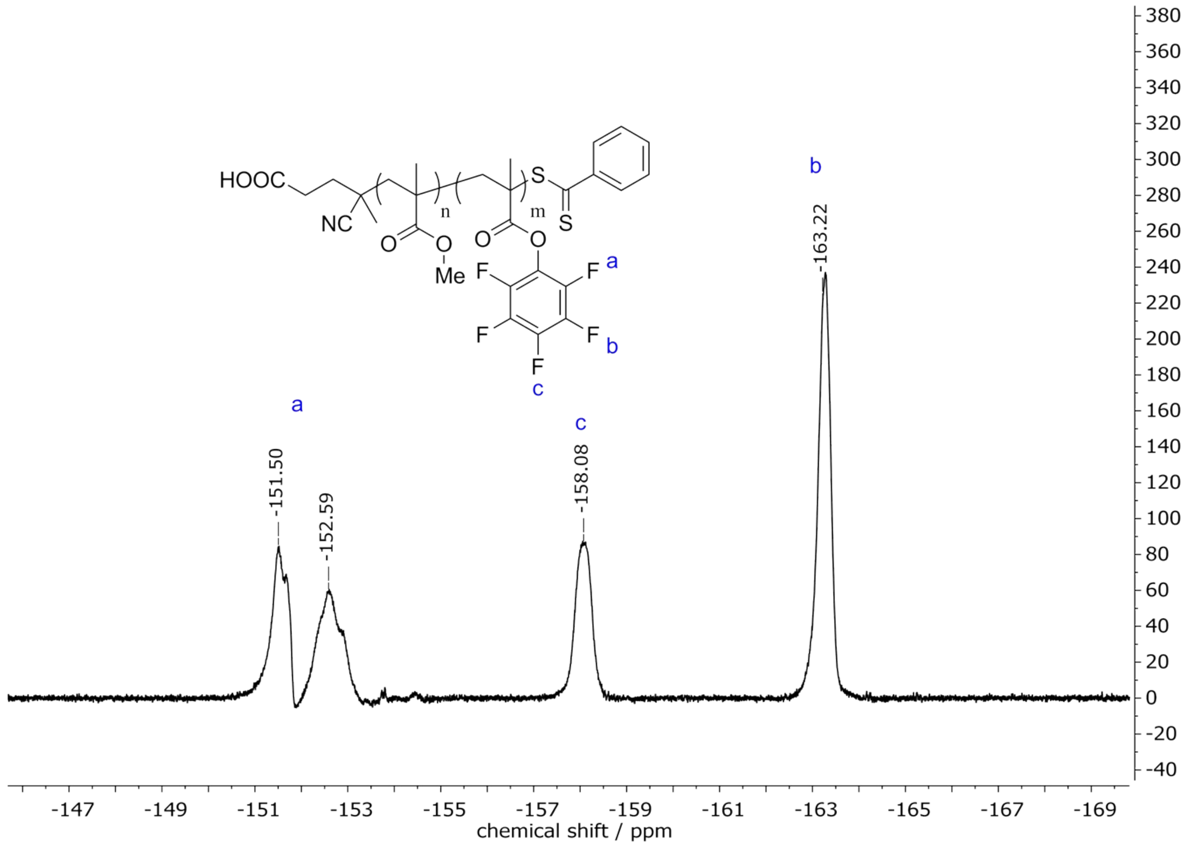

Figure S2: ^{19}F-NMR of reactive ester block copolymer P(MMA-*b*-PFPMA).

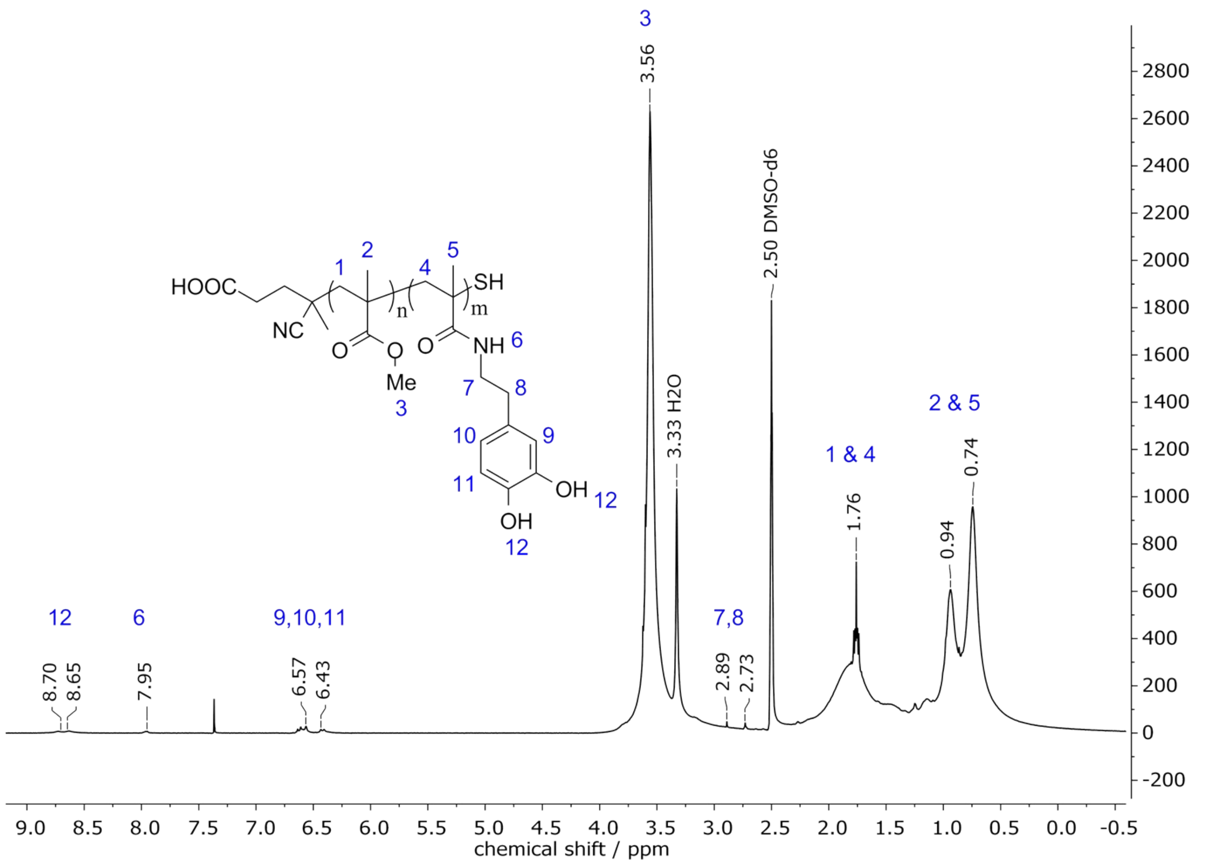

Figure S3: ^{1}H-NMR of anchor block copolymer P(MMA-*b*-DOPA). The ratio between the PMMA block and the DOPA-block was determined to be about 10:1 by using ref. 1, however this value is uncertain due to the overlap of the signal at 3.56 ppm with the residual water signal at 3.33 ppm.

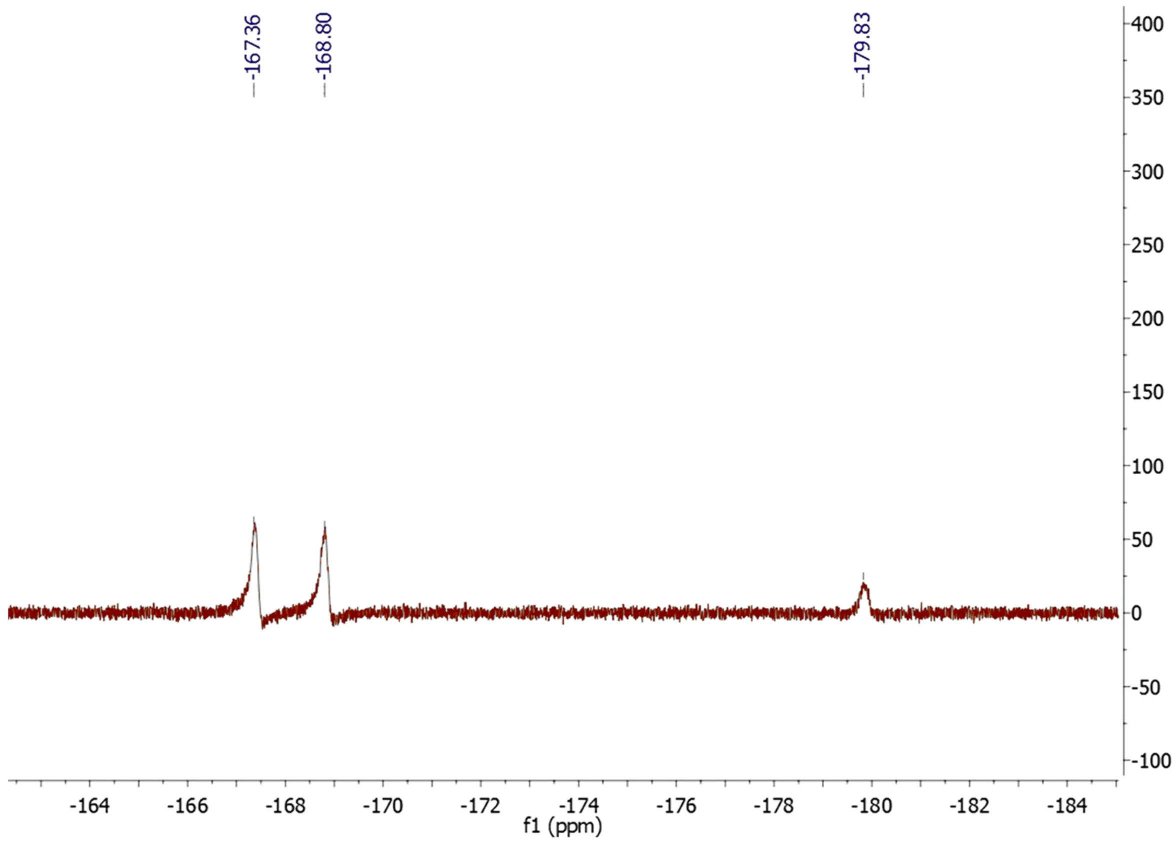

Figure S4: ^{19}F-NMR of anchor block copolymer P(MMA-*b*-DOPA) before purification (signals of pentafluorphenol are visible, but no signals for the reactive ester bonded pentaflourophenol, as showed in S2). After purification, no signals are visible anymore.

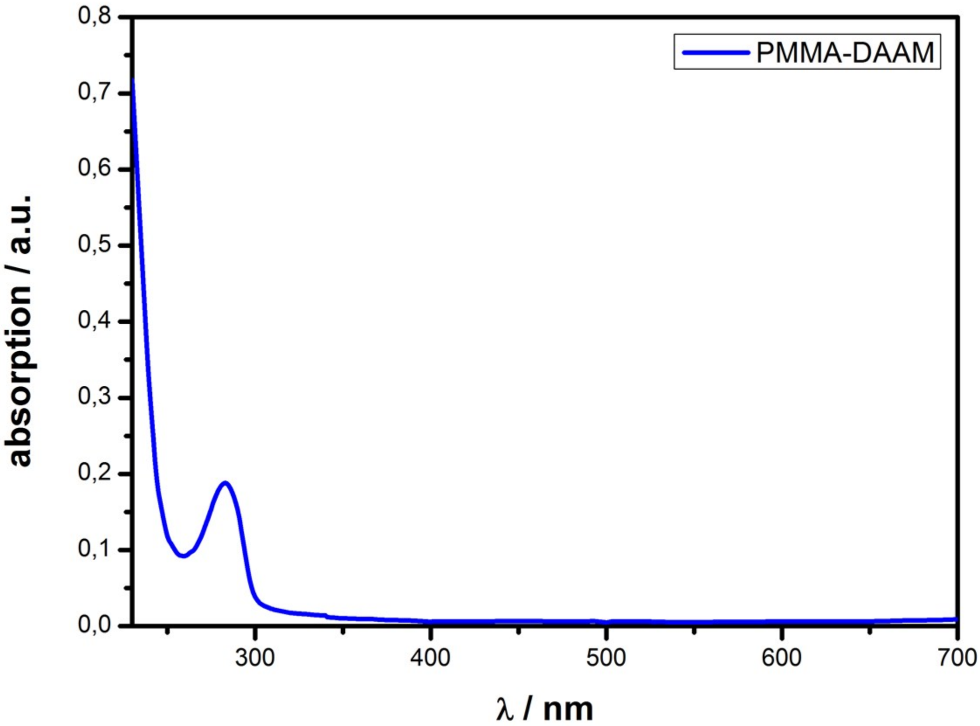

Figure S5: UV-vis-spectroscopy of block copolymer P(MMA-*b*-DAAM) showing an absorption band around 283 nm corresponding to the absorption of dopamine.

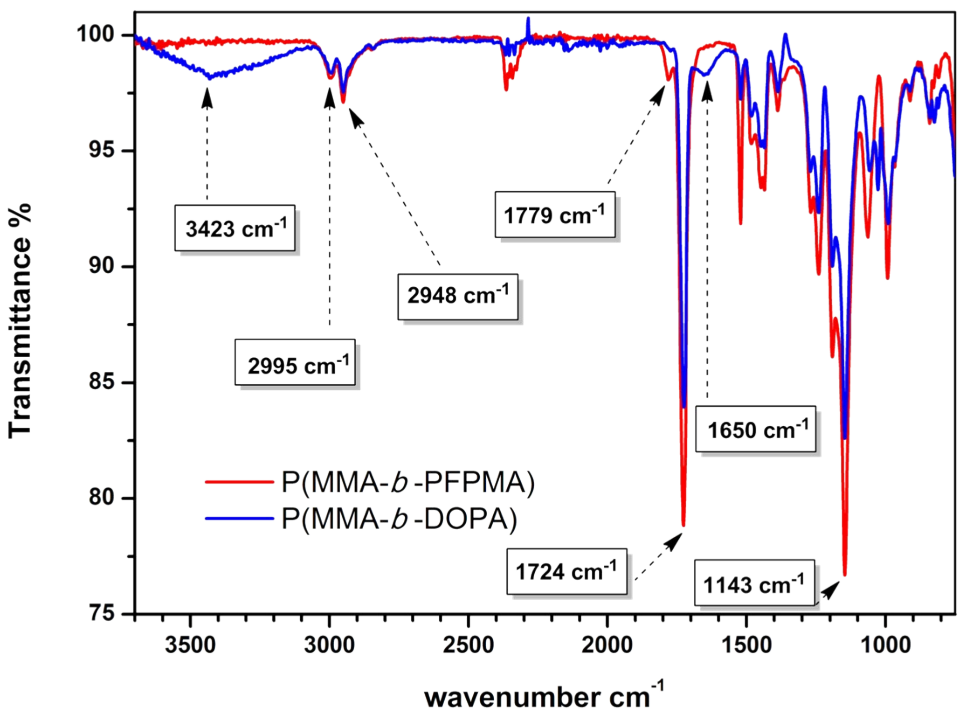

Figure S6: IR spectra of reactive block copolymer P(MMA-*b*-PFPMA) (red) and after polymer analogous reaction block copolymer (PMMA-*b*-DOPA). The successful attachment of the dopamine anchor group can be proven due to complete disappearance of the C=O band of the ester at 1779 cm^{-1} and the appearance of the C=O band of the corresponding amide at a wavenumber of 1650 cm^{-1}.

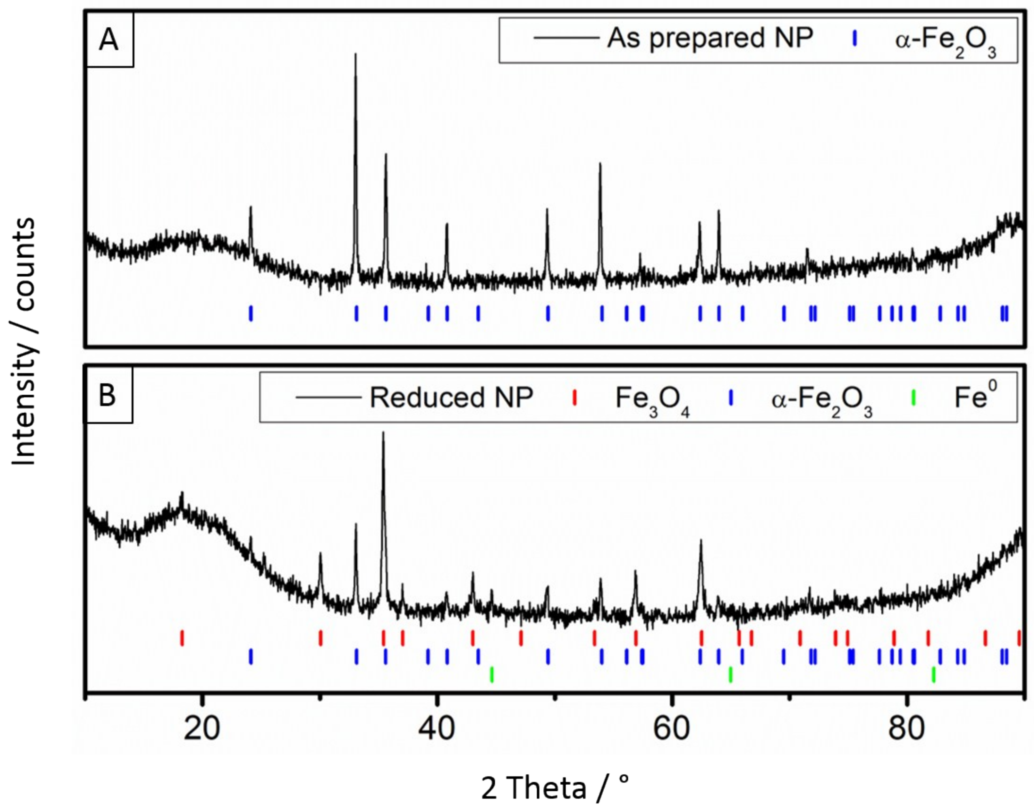

Figure S7: X-ray powder diffraction of precursor particles (black) and reflex position of reduced particles (blue). B: Diffraction pattern of reduced particles. Reflexes were assigned to hematite[2], magnetite[3] and iron (0).[4]

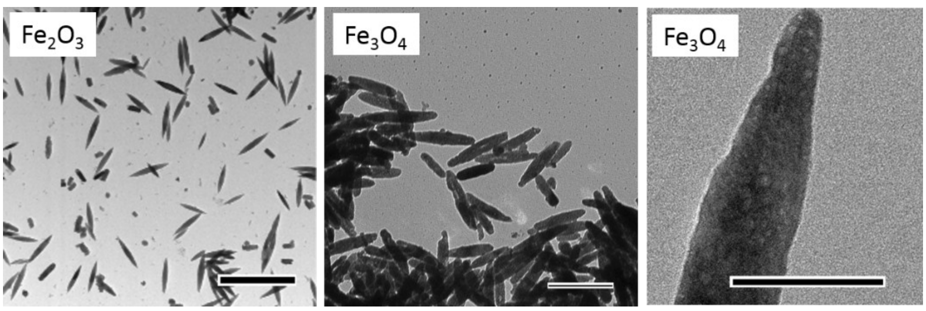

Figure S8: TEM images of the as prepared Fe_2O_3-particles (left) and the reduced particles (labled Fe_3O_4) with a higher magnification image to show the cavities formed by the Kirkendall-effect on the right.

Table S1: Size and magnetic properties of Fe_3O_4 nanorods.

compound	L_{long} / nm	L_{short} / nm	ratio	T_B / K	M_{Sat} / emu/g at 5 K (5 T)	M_{Sat} / emu/g at 300 K (5 T)	Remanence / emu/g at 5 K	Remanence / emu/g at 300 K	Coercitivity / Oe at 5 K	Coercitivity / Oe at 300 K
α-Fe_2O_3	428 (27 %)	87 (16 %)	~4,9	>300	2,0	0,8	0,09	0,07	950	450
Fe_3O_4	340 (30 %)	77 (27 %)	~4,4	>300	53,8	48,8	12	8	150	150

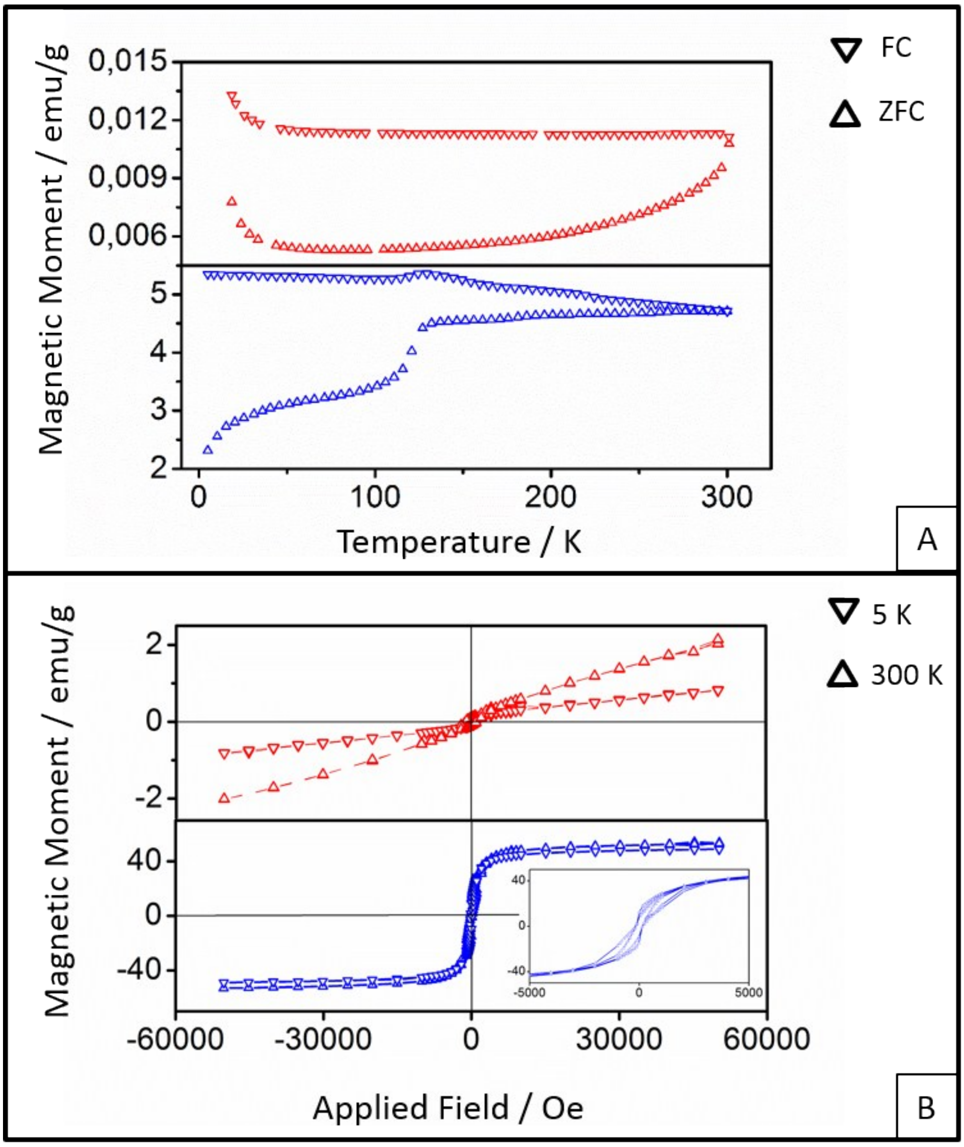

Figure S9: A shows the temperature-dependent magnetic moment of the particles. A-Fe_2O_3 precursor particles (red) exhibit a very small magnetic moment compared to the reduced particles (blue). B shows the magnetic moment against the applied field (Oe). Precursor particles (red) show weak ferromagnetic behaviour while the reduced particles are strongly magentic but show no significant hysteresis.

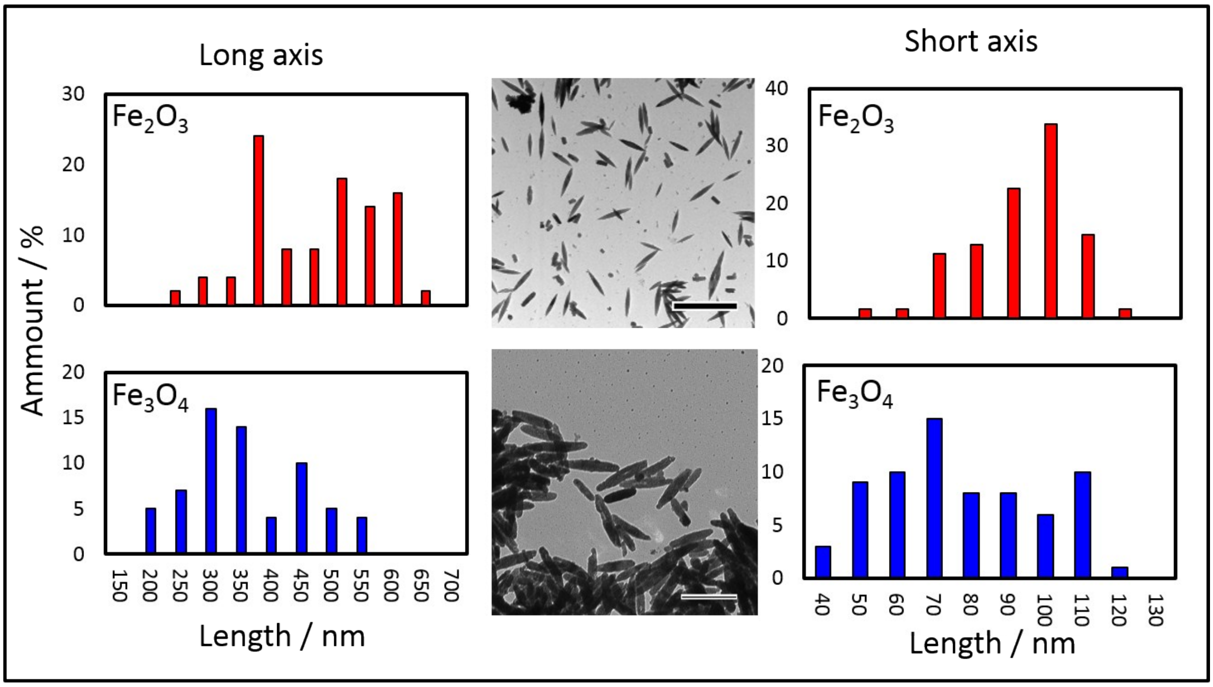

Figure S10: Size distribution of short and long axis of Fe_2O_3 precursor particles (red) and reduced particles (blue).

References

1 Q. Zhang, P. Schattling, P. Theato & R. Hoogenboom, Polymer Chemistry, 2012, 3(6), 1418-1426.

2 Pauling L, Hendricks S B, "The Structure of Hematite", Journal of the American Chemical Society 47, 781-790 (1925).

3 Claassen A A, "The scattering power of oxygen and iron for X-Rays", Proceedings of the Physical Society, London 38, 482-487 (1926)

4 Fe-5Al-20Ni(5to)0.1 ;COD (Crystallography Open Database); 11001087